

# Neural Network Based Pore Flow Field Prediction in Porous Media Using Super Resolution

Xu-Hui Zhou,<sup>1</sup> James McClure,<sup>2</sup> Cheng Chen,<sup>3,\*</sup> and Heng Xiao<sup>1,†</sup>

<sup>1</sup>*Kevin T. Crofton Department of Aerospace and Ocean Engineering, Virginia Tech, Blacksburg, Virginia, USA*

<sup>2</sup>*Advanced Research Computing, Virginia Tech, Blacksburg, Virginia, USA*

<sup>3</sup>*Department of Civil, Environmental and Ocean Engineering,  
Stevens Institute of Technology, Hoboken, New Jersey, USA*

Previous works have demonstrated using the geometry of the microstructure of porous media to predict the flow velocity fields therein based on neural networks. However, such schemes are purely based on geometric information without accounting for the physical constraints on the velocity fields such as that due to mass conservation. In this work, we propose using a super-resolution technique to enhance the velocity field prediction by utilizing coarse-mesh velocity fields, which are often available inexpensively but carry important physical constraints. We apply our method to predict velocity fields in complex porous media. The results demonstrate that incorporating the coarse-mesh flow field significantly improves the prediction accuracy of the fine-mesh flow field as compared to predictions that rely on geometric information alone. This study highlights the merits of including coarse-mesh flow field with physical constraints embedded in it.

## I. INTRODUCTION

Fluid flow through porous media is a pervasive physical phenomenon, which has critical implications and practical applications in a wide range of natural and engineered processes, such as geological carbon storage [1], oil and gas extraction [2], and contaminant management in groundwater [3, 4]. There are many different methods to simulate flow fields within the porous media. Among these, the most powerful and attractive methods are direct numerical simulation (DNS) methods because they directly solve the Navier-Stokes equations and provide the flow fields with highest accuracy at the pore scale, which can be implemented using the Lattice Boltzmann method (LBM) [5–7], finite volume method [8, 9] or finite element method [10, 11]. However, these methods are highly demanding in terms of computational time and memory requirements.

In recent years, machine learning, especially deep learning, has emerged as a promising tool in the scientific and engineering community. Deep learning, in the form of neural networks, is able to learn the physical relationship between a set of input and output data obtained from experiments or numerical simulations, which in turn helps predict the variables of interest in a fast and cost-effective manner. This technique has been successfully applied in a number of scientific fields, such as learning nonlocal constitutive models for transport PDEs [12] and learning potential energy surface for atomic and molecular systems [13].

For porous media, such method has been used to learn the mapping of the geometry of solid microstructure to

---

\* Corresponding author; chen08@vt.edu

† hengxiao@vt.edu

some critical physical properties such as the permeability. Among these works, Srisutthiyakorn [14] employed both multilayer neural network (MNN) and convolutional neural network (CNN) algorithms to predict the permeability based on 2-D/3-D geometric images, showing that multi-scale geometric features help the neural network capture global pore connections and improve the prediction capability. In addition to using pure binary geometric images as the input, Wu *et al.* [15] included features such as the porosity, defined as the ratio of void space volume to total sample volume, and specific surface area, defined as the solid-void interface area per unit sample volume, as the physical or geometric indicators in the CNN’s fully connected layers to enhance the accuracy of the permeability prediction. Compared to developing a surrogate model for the prediction of scalar-valued quantities, predicting the flow fields through the pore space in porous media is much more challenging. Ying *et al.* [16] developed and trained a gated U-net model to map geometric images to flow fields in both 2-D and 3-D domains. They showed that the prediction performance was highly susceptible to the complexity of the porous media with lower prediction accuracy in more complex pore structures. Conversely, they found that the predicted permeability was much less sensitive to the complexity of the pore structure. A similar CNN-based PoreFlow-Net model was introduced by Santos *et al.* [17] to predict the flow field at each voxel of the input of 3-D geometric image. Besides using the 3-D geometry as the input, they incorporated an additional physical feature, the time of flight (ToF), to inform the network about the global conditions of the domain. These studies all focused on developing and training an end-to-end neural network to predict the flow fields in the porous media without using any velocity data in the model inputs.

The CNN-based super-resolution technique, a method to enhance (i.e., increase) the resolution of an imaging system [18], has been developed to reconstruct high-resolution flow fields based on the low-resolution flow fields. Fukami *et al.* [19] applied this method to reconstruct the full-resolution DNS flow fields based on the low-resolution flow fields which were simply obtained by pooling of the DNS flow images. Liu *et al.* [20] developed a novel multiple temporal paths CNN and compared it to the traditional static CNN, showing that taking a temporal sequence of low-resolution snapshots as the input helped capture the non-local turbulent processes in both time and space. These studies showed that CNN-based super-resolution technique achieved progress in reconstruction of flow fields because the low-resolution flow fields imposed physical constraints on the prediction at a coarse level.

In light of the observations above, it seems natural to explore combining the geometric information with the low-resolution flow fields to obtain a better predicted flow fields with high resolution. In this work, we proposed a CNN-based neural network assisted with the super-resolution technique to predict the single-phase pore flow fields through the pore space in porous media. The sphere-packed porous media were generated as the porous media to be trained. The pore flow fields within the pore space of the porous media on both coarse and fine meshes were simulated using LBM, which were included into the database for training and testing the neural network. Specifically, the low-resolution velocity fields on coarse mesh grids can be simulated with a low computational cost because the mesh was coarsened by a factor of 4 in a single dimension based on the fine mesh, and we found that the computational time of simulating the low-resolution (i.e., coarse-resolution) pore flow field was less than 5% of that for simulating a high-resolution (i.e., full-resolution) pore flow field. Particularly, the well-trained neural network used the full-resolution pore geometry and coarse-resolution pore flow field as the model inputs and then predicted the full-resolution pore flow field as the model output. Through this study, we showed that incorporating additional information (i.e., coarse-resolution pore flow field) into the model input can improve the prediction performance and accuracy at a relatively low computational cost, especially for unseen pore geometries.

## II. METHODOLOGY

In this section, we present (1) the generation of training data and (2) the architecture of the proposed neural network. The generation of porous assemblies was implemented using the open-source SpherePackTools package [21], which can generate porous media packed with spheres having lognormally-distributed radii and provides control over the final porosity of the porous medium. The size of generated porous assemblies was  $L_x = L_y = L_z = 1.0$ . In each porous medium, the number of spheres and variance of sphere radius for were set as  $N_s = 1000$  and  $\sigma^2 = 0.1$ , respectively. The target porosity,  $\phi_{target}$ , was set within the range of  $[0.25, 0.35]$  to generate five different porous assemblies for training. Among these, packings of sphere in two porous assemblies were removed from the center to mimic the porous medium with a large vuggy pore space, which is shown in Fig. 1.

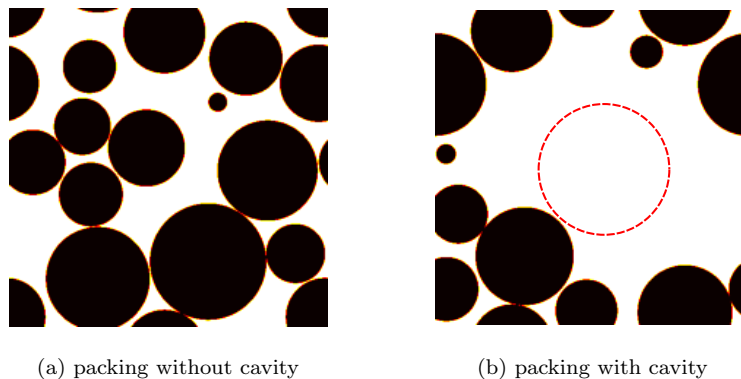


FIG. 1: Cross-sections of two different porous assemblies used for training: fully-packed assembly (left panel) and assembly with vuggy pore space inside (right panel). The assembly with vuggy pore space is obtained by removing the spheres overlapping with the central spherical area (the red dotted circle) from a fully-packed assembly.

Direct numerical simulation of the steady-state pore flow field within the pore space was conducted using the multi-relaxation time (MRT) lattice Boltzmann method (LBM), which was implemented through the open-source LBPM software package [22]. For stationary, creeping, incompressible flow in porous media, the Navier-Stokes equation simplifies to the Stokes equation  $\mu \nabla^2 \mathbf{u} - \nabla p + \rho \mathbf{g} = 0$ , where  $\nabla p = 0$  in our periodic system. To remove the effects of using different resolution, the Stokes equation was non-dimensionalized by a factor of  $D^3/\mu^2$ :

$$0 = \frac{D^3}{\mu^2} (\mu \nabla^2 \mathbf{u} + \rho \mathbf{g}) = D^2 \nabla^2 \left( \frac{\mathbf{u} D}{\mu} \right) + \frac{\rho \mathbf{g} D^3}{\mu^2}$$

where the Reynolds number is  $\text{Re} = \frac{\mathbf{u} D}{\mu}$  and  $D$  is the Sauter mean grain diameter.

In the MRT approach, the relaxation time, which controls fluid viscosity, is set as  $\tau = 1.0$ , and the external body force is applied only in the  $z$  direction with  $\mathbf{g}_z = 10^{-4}$  for high resolution and  $\mathbf{g}_z = 6.4 \times 10^{-3}$  for coarse resolution. When simulating the high-resolution pore flow fields, the number of lattice nodes in the domain were  $n_x = n_y = n_z = 512$ . In comparison, the number of lattice nodes in each direction was changed to 128 when simulating the coarse-resolution pore flow fields. Each porous assembly was evenly segmented into 64 subassemblies and we had 320 porous assemblies in total as the training dataset.

In this study, we proposed a convolutional neural network to predict the high-resolution pore flow field in a porous

medium based on: (1) high-resolution pore geometry, and (2) low-resolution pore flow field, which is illustrated in Fig. 2.

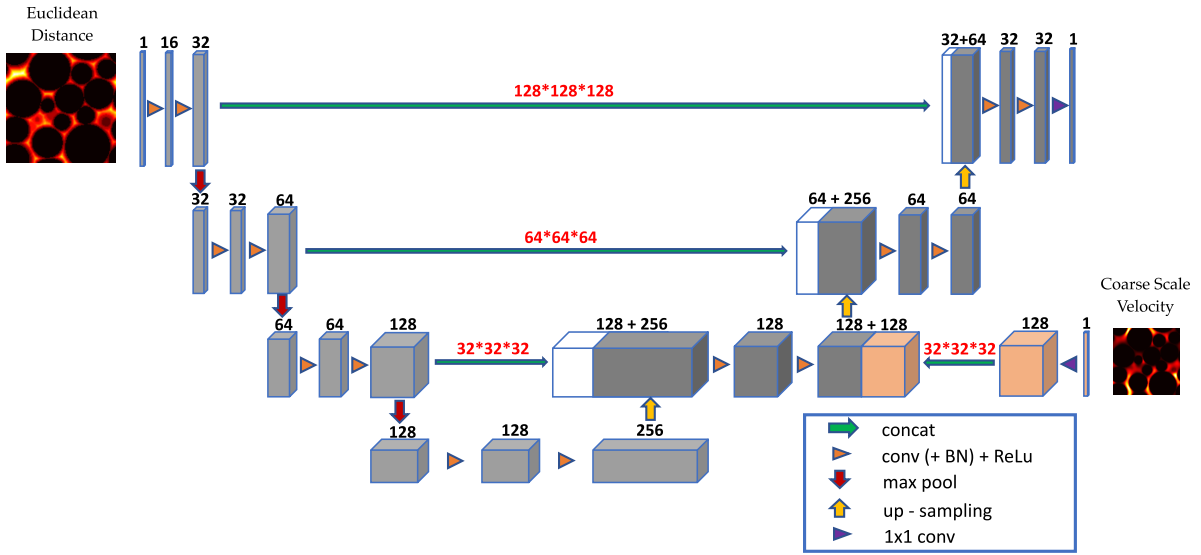


FIG. 2: Schematic plot of the U-net based neural network assisted with the super-resolution technique, which predicts high-resolution pore flow fields in porous media based on low-resolution pore flow fields and high-resolution pore geometry data. Particularly, a high-resolution ( $128 \times 128 \times 128$ ) 3-D Euclidean distance map and low-resolution ( $32 \times 32 \times 32$ ) 3-D pore flow field are used as the model inputs, and the model output is a high-resolution ( $128 \times 128 \times 128$ ) 3-D pore flow field in the pore space of the porous medium. The gray boxes represent feature maps and the white boxes represent the copied features mapped from the left, encoder part. The orange boxes represent feature maps from the coarse-resolution pore flow field. The number of information channels is denoted above each feature map. The dimensions of 3-D images on each level are denoted above the concatenation arrows. Arrows with different colors denote different operations.

Similar to the standard U-net model [23], the proposed network consists of a contracting path (left) and an expansive path (right), each with four resolution steps. In the contracting path, the 3-D image resolution is reduced whereas the information channel number is enhanced, which enables extraction of the pore geometry features. Specifically, each convolutional layer consists of two  $3 \times 3 \times 3$  convolutional filters and doubles the number of feature channels followed by a max-pooling layer consisting of a  $2 \times 2 \times 2$  filter that coarsens the image resolution by a factor of two in each dimension. In the expansive path, each upsampling layer of the ‘nearest’ mode doubles the resolution of feature maps in each single dimension followed by a concatenation with the corresponding feature maps of the same resolution from the left, contracting path; each convolutional layer consists of two  $3 \times 3 \times 3$  convolution filters and reduces the the number of feature channels. The concatenations aim to reuse the features by concatenating them to the layers of the same resolution in the right, decoder part, which allows for more geometric information to be retained. In the last layer, a  $1 \times 1 \times 1$  convolution filter is used to reduce the number of output channels to the number of label channels which equals to one in our case. In the neural network, we selected the rectified linear activation function (ReLU) as the activation function because it is easy to train and often achieves good performance. In addition, we used batch

normalization (BN) [24] before each ReLU operation, which standardizes the inputs to a layer for each batch and accelerates the training process.

Inspired by the super-resolution technique, we concatenated a low-resolution 3-D pore flow field to the 3-D geometric map in the expansive path, which helps construct the pore flow field at a higher resolution. Specifically, the coarse-resolution pore flow field is fed into a  $1 \times 1 \times 1$  convolutional layer to increase the number of feature maps from 1 to 128, which equals to the number of the feature channels of the 3-D geometric map in the expansive path. In this way, we assume that the geometric information and coarse-resolution pore flow field are of equal importance for the final prediction of the high-resolution pore flow field.

We used the high-resolution ( $128 \times 128 \times 128$ ) Euclidean distance map of segmented subassembly as the input of pore geometry whereas the input of the pore flow field is in the coarse resolution ( $32 \times 32 \times 32$ ). The model output of the predicted pore flow field is in the high resolution ( $128 \times 128 \times 128$ ). The proposed neural network model was implemented and then trained using PyTorch [25], a machine learning library. The Adam optimizer was adopted to train the neural network model. The training process took 600 epochs with a batch size of 16. The training was scheduled such that the learning rate was initialized as 0.001 and then reduced by multiplying a factor of 0.7 every 200 epochs.

### III. RESULTS

After training, the model was tested to predict the flow fields in two different porous media which were not included in the training dataset. The first testing experiment involved a fully-packed porous medium. We can see that both the predicted pore flow fields given by the trained model with and without the input of coarse-resolution flow fields are close to the ground-truth pore flow field, which is shown in the top row in Fig. 3. The prediction error is 5.7% using the coarse-resolution pore flow field as model input. Conversely, it is 9.2% without using the coarse-resolution pore flow field as model input. This suggested the advantage of incorporating the coarse-resolution pore flow field into model inputs. However, it is clear that the difference in the two prediction accuracy values is relatively small. This is because the testing dataset is a collection of fully-packed spherical particles, which is highly similar to most of the samples in the training dataset, leading to a small generalization error for the model even without using the coarse-resolution pore flow field data in model input.

The second testing experiment involved the porous medium with a cavity (i.e., a large vuggy pore space) in the domain center to investigate the effect of using the coarse-resolution flow field as a model input. This testing experiment is highly relevant to hydrocarbon energy recovery in carbonate reservoirs, because carbonate rocks are rich in large fractures and vuggy pores, leading to challenges in direct, coupled simulations of Stokes flow and Darcy flow in the vuggy pore space and rock matrix, respectively. It is clear that the pore flow field prediction using the coarse-resolution pore flow field as a model input is much closer to the corresponding ground truth compared to the prediction using pure geometry images in model inputs, which is shown in the bottom row in Fig. 3. The prediction error is 11.7% using the coarse-resolution pore flow field as model input. But it increases dramatically to 40.1% without using the coarse-resolution pore flow field as model input. Compared to the prediction using the coarse-resolution pore flow field as a model input, the prediction without using the coarse flow field data demonstrated non-physical velocity discontinuity near the center of the vuggy pore space, due to the lack of physics information in

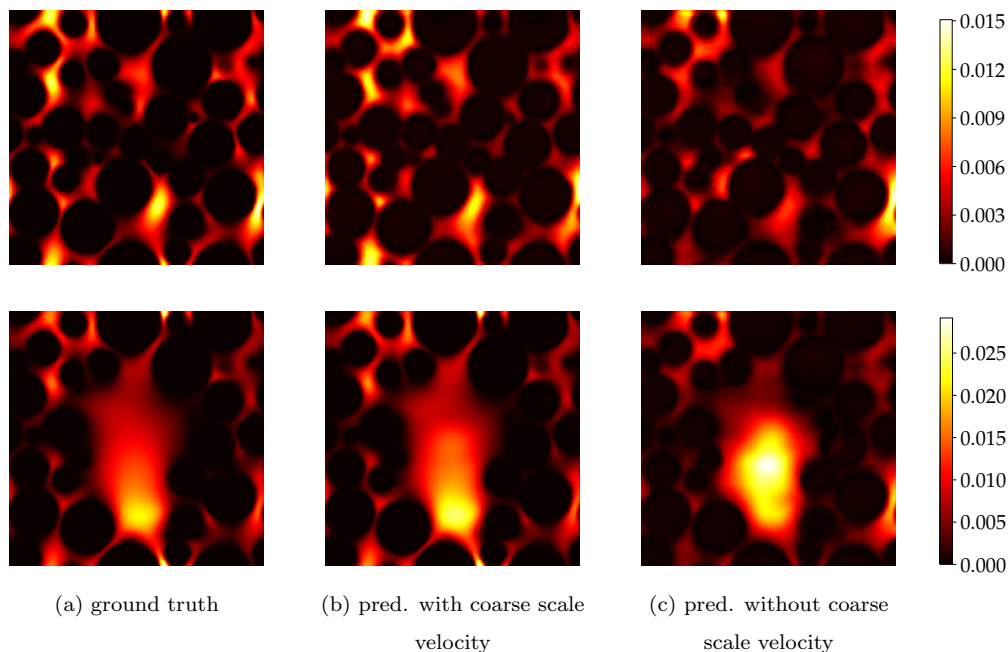


FIG. 3: a) Ground-truth pore flow field and the corresponding predictions b) with and c) without using the coarse-resolution pore flow field as a model input. The top row is for a fully-packed porous medium and the bottom row is for a porous medium with a cavity (i.e. a large vuggy pore space) inside. Both ground truths and predictions are in the 3-D space, and in this figure 2D cross-sectional pore flow fields are demonstrated for easy comparison.

the model input. The comparison in the second testing experiment illustrated the advantage of our physics-informed neural network model: the inclusion of a coarse-resolution pore flow field in the model input, which can be obtained with relatively low computational costs, significantly reduces the generalization error of the model when it works on an unseen sample.

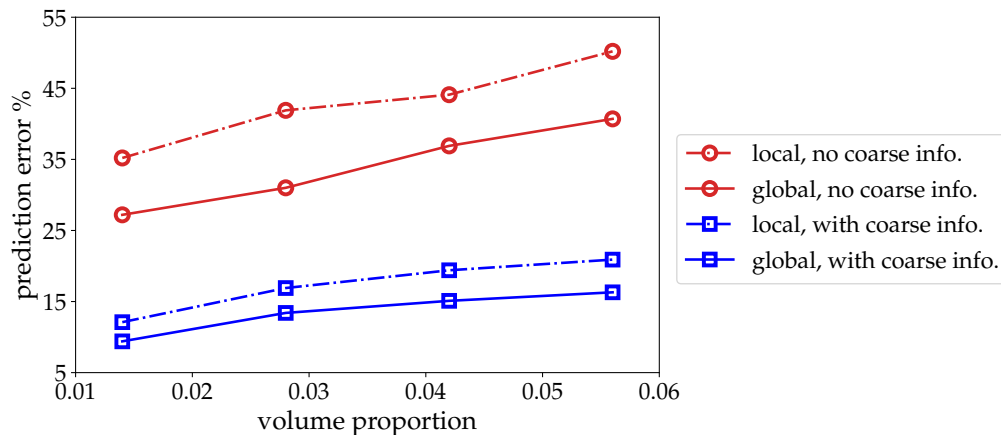


FIG. 4: The prediction errors at various volume proportions. The solid and dashed lines represent the prediction errors for the whole porous medium and the large vuggy regions, respectively. The blue and red lines represent the prediction errors with and without low-resolution flow fields, respectively.

We use four porous media with varying large vuggy volumes to evaluate the prediction performance of the trained neural networks. The prediction errors of testing porous media are shown in Fig. 4. The volume proportion represents the ratio of the inner large spherical vuggy volume to that of the whole porous medium. We calculate the prediction errors for two domains: (1) local error for large vuggy regions and (2) global error for the whole porous medium. We can see that the local errors are larger but close to the global errors and both errors get larger with volume proportion increasing, which means the large vuggy pores are the main sources of prediction errors. Such prediction errors are significantly reduced when incorporating the low-resolution flow field as a model input, which again shows the advantage of imposing physical constraints by using coarse flow field.

#### IV. CONCLUSIONS

Simulating the flow fields in porous media at the pore scale is usually expensive and time-consuming. Drawing inspirations from the super-resolution technique, in this work we proposed a CNN-based neural network assisted with the low-resolution flow fields to quickly predict the high-resolution flow fields in the porous media. Such a neural network can enhance the accuracy of predicted flow fields in the porous media with a low computational cost, especially for the porous media different from those in the training dataset. Incorporating coarse-mesh physical information as an input feature for neural networks is a promising strategy for predicting fields with non-local physics.

- 
- [1] M. J. Blunt, B. Bijeljic, H. Dong, O. Gharbi, S. Iglauer, P. Mostaghimi, A. Paluszny, and C. Pentland, Pore-scale imaging and modelling, *Advances in Water Resources* **51**, 197 (2013).
  - [2] J. Bear, *Dynamics of Fluids in Porous Media* (Courier, 2013).
  - [3] M. Hilpert and C. T. Miller, Pore-morphology-based simulation of drainage in totally wetting porous media, *Advances in water resources* **24**, 243 (2001).
  - [4] Q. Kang, P. C. Lichtner, and D. Zhang, An improved lattice boltzmann model for multicomponent reactive transport in porous media at the pore scale, *Water Resources Research* **43** (2007).
  - [5] J. E. McClure, J. F. Prins, and C. T. Miller, A novel heterogeneous algorithm to simulate multiphase flow in porous media on multicore CPU-GPU systems, *Computer Physics Communications* **185**, 1865 (2014).
  - [6] M. A. Spaid and F. R. Phelan Jr, Lattice Boltzmann methods for modeling microscale flow in fibrous porous media, *Physics of Fluids* **9**, 2468 (1997).
  - [7] E. S. Boek and M. Venturoli, Lattice-boltzmann studies of fluid flow in porous media with realistic rock geometries, *Computers & Mathematics with Applications* **59**, 2305 (2010).
  - [8] P. Jenny, S. Lee, and H. A. Tchelepi, Multi-scale finite-volume method for elliptic problems in subsurface flow simulation, *Journal of Computational Physics* **187**, 47 (2003).
  - [9] Y. Song, K. Chung, T. Kang, and J. Youn, Prediction of permeability tensor for three dimensional circular braided preform by applying a finite volume method to a unit cell, *Composites Science and Technology* **64**, 1629 (2004).
  - [10] Z. Sun, R. E. Logé, and M. Bernacki, 3D finite element model of semi-solid permeability in an equiaxed granular structure, *Computational materials science* **49**, 158 (2010).
  - [11] C. Sandino, P. Krociczek, D. D. McErlain, and S. K. Boyd, Predicting the permeability of trabecular bone by micro-computed tomography and finite element modeling, *Journal of biomechanics* **47**, 3129 (2014).

- [12] X.-H. Zhou, J. Han, and H. Xiao, Learning nonlocal constitutive models with neural networks, *Computer Methods in Applied Mechanics and Engineering* **384**, 113927 (2021).
- [13] J. Han, L. Zhang, R. Car, *et al.*, Deep potential: A general representation of a many-body potential energy surface, arXiv preprint arXiv:1707.01478 (2017).
- [14] N. Srisutthiyakorn, Deep-learning methods for predicting permeability from 2d/3d binary-segmented images, in *SEG technical program expanded abstracts 2016* (Society of Exploration Geophysicists, 2016) pp. 3042–3046.
- [15] J. Wu, X. Yin, and H. Xiao, Seeing permeability from images: fast prediction with convolutional neural networks, *Science bulletin* **63**, 1215 (2018).
- [16] D. W. Ying, T. Chung, R. T. Armstrong, and P. Mostaghimi, MI-lbm: Machine learning aided flow simulation in porous media, arXiv preprint arXiv:2004.11675 (2020).
- [17] J. E. Santos, D. Xu, H. Jo, C. J. Landry, M. Prodanović, and M. J. Pyrcz, PoreFlow-Net: A 3D convolutional neural network to predict fluid flow through porous media, *Advances in Water Resources* **138**, 103539 (2020).
- [18] C. Dong, C. C. Loy, K. He, and X. Tang, Image super-resolution using deep convolutional networks, *IEEE transactions on pattern analysis and machine intelligence* **38**, 295 (2015).
- [19] K. Fukami, K. Fukagata, and K. Taira, Super-resolution reconstruction of turbulent flows with machine learning, *Journal of Fluid Mechanics* **870**, 106 (2019).
- [20] B. Liu, J. Tang, H. Huang, and X.-Y. Lu, Deep learning methods for super-resolution reconstruction of turbulent flows, *Physics of Fluids* **32**, 025105 (2020).
- [21] J. E. McClure, Spherepacktools, <https://github.com/JamesEMcClure/SpherePackTools> ().
- [22] J. E. McClure, Lbpm, <https://github.com/OPM/LBPM> ().
- [23] O. Ronneberger, P. Fischer, and T. Brox, U-net: Convolutional networks for biomedical image segmentation, in *International Conference on Medical image computing and computer-assisted intervention* (Springer, 2015) pp. 234–241.
- [24] S. Ioffe and C. Szegedy, Batch normalization: Accelerating deep network training by reducing internal covariate shift, in *International conference on machine learning* (PMLR, 2015) pp. 448–456.
- [25] A. Paszke, S. Gross, F. Massa, A. Lerer, J. Bradbury, G. Chanan, T. Killeen, Z. Lin, N. Gimelshein, L. Antiga, *et al.*, Pytorch: An imperative style, high-performance deep learning library, in *Advances in neural information processing systems* (2019) pp. 8026–8037.